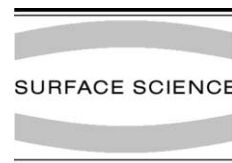




ELSEVIER

Surface Science 514 (2002) 249–255



www.elsevier.com/locate/susc

Pd₁/MgO(100): a model system in nanocatalysis

S. Abbet^{a,*}, A.M. Ferrari^b, L. Giordano^c, G. Pacchioni^c, H. Häkkinen^d,
U. Landman^d, U. Heiz^e

^a *Institut de Physique de la Matière Condensée, Université de Lausanne, CH-1015 Lausanne, Switzerland*

^b *Dipartimento di Chimica IFM, Università di Torino, via P. Giuria 5, I-10125 Torino, Italy*

^c *Dipartimento di Scienza dei Materiali, Istituto Nazionale per la Fisica della Materia, Università di Milano-Bicocca, via R. Cozzi 53, I-20125 Milano, Italy*

^d *School of Physics, Georgia Institute of Technology, Atlanta, GA 30332-0430, USA*

^e *Abteilung für Oberflächenchemie und Katalyse, Universität Ulm, D-89069 Ulm, Germany*

Received 26 September 2001; accepted for publication 1 March 2002

Abstract

Nanocatalysts consist of small size-selected clusters adsorbed on uniform sites of a support material. Here, we focus on a simple model system, which is fabricated by soft-landing atomic Pd ions on oxygen vacancies (F-centers) of a MgO(100) surface (Pd₁/MgO(F_s)). We used thermal desorption and infrared spectroscopies (TDS, FTIR) to study the acetylene polymerization and the CO oxidation catalyzed by this system. In one-heating-cycle experiments, only the formation of benzene is observed during the polymerization reaction and the combustion of CO leads to the formation of CO₂ detected at 260 and 500 K. Experimental results in combination with ab initio calculations reveal the mechanisms of these reactions and demonstrate the role of surface defects in nanocatalysis.

© 2002 Elsevier Science B.V. All rights reserved.

Keywords: Density functional calculations; Thermal desorption spectroscopy; Catalysis; Surface chemical reaction; Palladium; Magnesium oxides; Alkynes; Carbon monoxide

1. Introduction

Molecular-scale understanding of the energetics and mechanisms of catalytic reactions could open new avenues to the design of catalysts with specific functions [1,2]. In this respect nanocatalysts consisting of small size-selected clusters on uniform adsorption sites may be of special interest as small

clusters reveal distinct quantum size effects manifested, e.g., in the strong size-dependent chemical reactivity of gas-phase clusters [3–7]. In addition, these small clusters reveal a distinct interaction with the substrate and are highly fluxional. Recent experimental and theoretical joint studies revealed e.g. the reaction mechanism of the oxidation of CO on Au₈ clusters [8] and Pd atoms [9] and the polymerization of acetylene on Pd_n clusters [10].

In this paper we focus on the chemical reactivity of palladium atoms adsorbed on oxygen vacancies of a MgO(100) thin film and we summarize and compare the reaction mechanisms of the acetylene

* Corresponding author. Tel.: +41-21-692-36-53/87; fax: +41-21-692-36-35.

E-mail address: stephane.abbet@ipmc.unil.ch (S. Abbet).

polymerization and the CO oxidation on this model nanocatalyst. A palladium atom adsorbed on an F-center is highly selective for the cyclotrimerization of acetylene and forms CO_2 via two reaction mechanisms with $\text{Pd}(\text{CO})_2(\text{O}_2)$ and $\text{Pd}(\text{CO}_3)(\text{CO})$ as precursors.

2. Experimental

The palladium atoms are produced by a recently developed high-frequency laser evaporation source [11]. The positively charged ions are guided by home-built ion optics through differentially pumped vacuum chambers and are size-selected by a quadrupole mass spectrometer (Extranuclear C50/mass limit: 4000 amu). We deposited only 0.5% of a monolayer Pd atoms (1 ML = 2.25×10^{15} clusters/cm²) at 90 K with low kinetic energy in order to land them isolated on the surface and

to prevent agglomeration on the MgO films. The presence of isolated atoms/clusters is confirmed experimentally and theoretically. Experimentally we used nickel atoms/clusters as it is well known that they form stable metalcarbonyls. This carbonyl formation of small deposited Ni_n ($n = 1-3$) was studied by exposing the deposited clusters to carbon monoxide. Mass spectrometry experiments showed that the nuclearity of the formed Ni_n carbonyls ($n = 1-3$) is not changed [12]. The absence of, for example, $\text{Ni}_1(\text{CO})_4$ and $\text{Ni}_3(\text{CO})$ after deposition of Ni_2 directly excludes fragmentation and agglomeration (Fig. 1a/b). Second, Monte Carlo simulations revealed that under our experimental conditions, e.g. atom flux ($\sim 10^9$ cm⁻¹), atom density ($\sim 10^{13}$ cm⁻¹), and defect density ($\sim 5 \times 10^{13}$ cm⁻¹) on the MgO(100) films <10% of the atoms coalesce when migrating to the trapping centers. The support is prepared in situ for each experiment; thin films are epitaxially grown on a

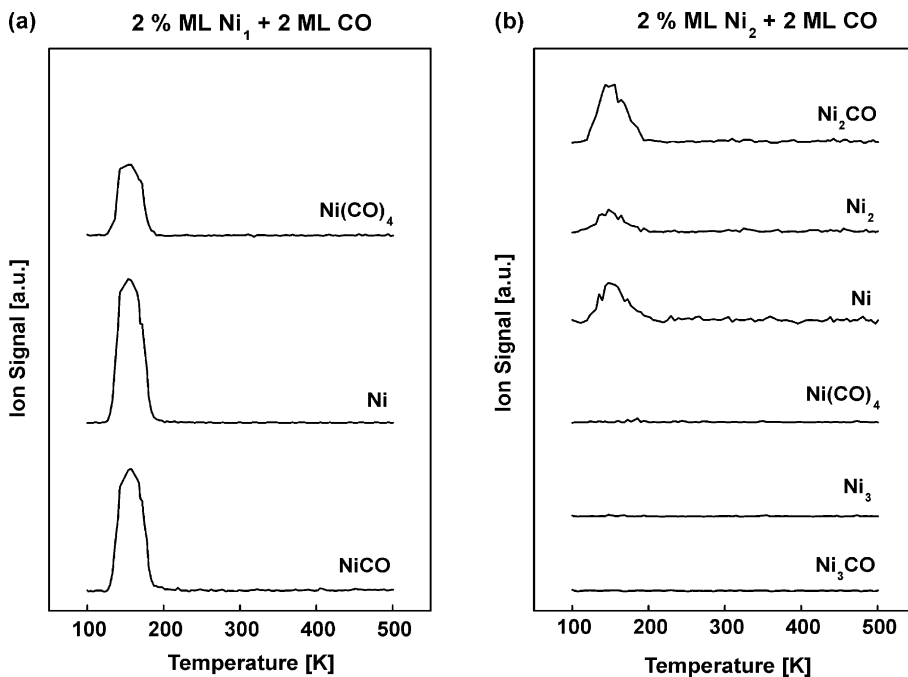


Fig. 1. (a) Thermal desorption spectra after deposition 2% of a monolayer of Ni atoms on MgO thin films and exposing the sample to 2 ML CO. These results show that $\text{Ni}(\text{CO})_4$ is formed on the surface. The Ni and NiCO species are fragmentation products during ionization of $\text{Ni}(\text{CO})_4$ in the mass spectrometer. (b) Thermal desorption spectra after deposition 2% of a monolayer of Ni_2 on the MgO thin films and exposing the sample to 2 ML CO. Shown are representative species. It is interesting to note that no $\text{Ni}(\text{CO})_4$ - and Ni_3 -containing species are detected. This indicates that at these experimental conditions no Ni atoms and trimers are present on the surface.

Mo(100) surface by evaporating magnesium in a $^{16}\text{O}_2$ background [13] and subsequently annealing the oxide film to 1000 K. These films show bulk-like properties. However, small amounts of defects like steps, kinks and F-centers are detected by the desorption behavior of small molecules [14].

For the cyclotrimerization and CO oxidation on Pd atoms we first exposed, using a calibrated molecular beam doser, the prepared model catalysts at 90 K to about 1 Langmuir (L) of acetylene or 1 L of $^{18}\text{O}_2$ and ^{13}CO , respectively. In a temperature programmed reaction (TPR) study, catalytically formed benzene (C_6H_6), butadiene (C_4H_6) and butene (C_4H_8) or $^{13}\text{C}^{18}\text{O}^{16}\text{O}$ molecules were detected by a mass spectrometer (BALZERS QMG 421) and monitored as function of temperature. It is interesting to note, that the reactants (^{13}CO , $^{18}\text{O}_2$, C_2H_2) are only physisorbed on the cluster-free MgO. This means that the MgO support is not catalytically active. In addition, the interaction of the product molecules with the model catalysts were also studied and are described in Ref. [15].

The thermal stabilities of the deposited Pd atoms were investigated by Fourier transform infrared spectroscopy, which are found not to migrate up to around 300 K, because up to this temperature the vibrational frequency of adsorbed CO is not changing [15]. This rather high stability can be explained by the high binding energy (~ 3.5 eV) of Pd atoms bound to the F-centers [16].

3. Results and discussion

3.1. Acetylene polymerization

Surprisingly already a single Pd atom catalyzes the cyclotrimerization reaction and the benzene molecule (C_6H_6) is desorbing at 300 K. No other product molecules of the polymerization reaction (e.g. C_4H_6 , C_4H_8) are observed (Fig. 2a). Thus this model catalyst is highly selective for the cyclotrimerization reaction. We note that on a clean MgO(100) surface none of the products is formed (Fig. 2b).

To rationalize this result, density functional theory calculations have been performed and Gaussian-type basis sets were employed to construct the Kohn–Sham orbitals. For the Mg and O atoms of the clusters we used the all electron 6-31G basis set [17]; the Pd atoms were treated with the 18-electrons ECP of Hay and Wadt [18]. Here we used the gradient-corrected B3LYP (Becke’s-3 exchange functional [19] in combination with Lee–Yang–Parr correlation functional [20]) or BP functionals (Becke’s exchange functional [21] in combination with Perdew’s correlation functional [22]). For further computational details see Refs. [15,16,23]. The MgO(100) surface was represented by cluster models [24,25], an approach which has been found to accurately reproduce the electronic structure and the binding properties of surface complexes. Due to the highly ionic nature of MgO,

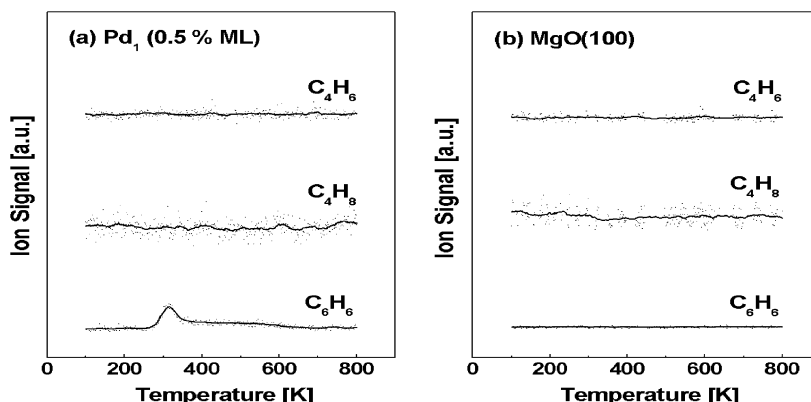


Fig. 2. (a) TPR spectra of the catalytic formation of C_6H_6 , C_4H_8 , and C_4H_6 on a Pd₁/MgO(100) sample. (b) Note that clean MgO(100) films do not catalyze the formation of these products.

the truncation of the lattice in cluster calculations implies the use of an external field to represent the long-range Coulomb potential. The model clusters considered have been embedded in arrays of point charges ($PC = \pm 2e$) and effective core potentials in order to reproduce the correct Madelung potential at the adsorption site under study. The morphological defects and the F-centers have been described by various sets of cluster models. The positions of the surface oxide anion, of the supported metal atoms and adsorbed molecules have been optimized using analytical energy gradients. The calculations have been performed with the Gaussian 98 program package [26].

In contrast to single crystal studies, suggesting an ensemble of a minimum number of Pd atoms necessary for the reaction [27], already a single Pd atom adsorbed on MgO is sufficient to catalyze the cyclotrimerization reaction. This surprising result can be rationalized by studying theoretically a palladium atom adsorbed on different MgO sites represented by a cluster of ions embedded in an array of point charges. First a Pd atom was adsorbed on a five-coordinated oxygen ion on the MgO(1 0 0) terrace, O_{5c} , the binding energy is about 1 eV. It was found that indeed the Pd(C_4H_4) complex is formed but the third acetylene molecule is not bound to the complex and therefore this configuration is catalytically inactive. Other bonding sites for the adsorption of Pd atoms are considered. On four-coordinated step or three-coordinated corner oxygen sites, O_{4c} and O_{3c} , respectively, the Pd atom binds slightly stronger with an energy of 1.2–1.5 eV, in addition, the atom is more reactive. However, on both O_{3c} and O_{4c} sites the third C_2H_2 molecule is only weakly bound or even unbound to the Pd(C_4H_4) surface complex, with the binding energy smaller than the activation energy of the formation of C_6H_6 . Thus, Pd atoms adsorbed on O_{nc} sites cannot explain the observed activity. This is consistent with the results of a recent experimental–theoretical study on the adsorption properties of CO on Pd₁/MgO [15], as the experimental results have been rationalized in terms of Pd atoms which are stabilized on oxygen vacancies (F-centers) in neutral or charged states, F_s or F_s^+ , respectively. The interaction of a Pd atom with the F-center is much stronger, 3.4 eV, which makes

these centers good candidates for Pd binding. On F_s^+ centers binding energies of about 2 eV have been computed [15]. The presence of trapped electrons at the defect site results in a more efficient activation of the supported Pd atom. In fact, the complex $(C_4H_4)(C_2H_2)/Pd_1/F_{5c}$ shows a large distortion and a strong interaction of the third C_2H_2 molecule. These results indicate that F- and F^+ -centers can act as basic sites on the MgO surface and turn the inactive Pd atom into an active catalyst. Notice that the supported Pd atoms on defect sites not only activate the cyclization reaction, but also favors benzene desorption, as shown by the very small $(C_6H_6)/Pd_1/F_{5c}$ adsorption energy. The complete reaction path for this specific nanocatalyst is shown in Fig. 3. The first barrier of the reaction path is the one for the formation of the intermediate Pd C_4H_4 and it is 0.48 eV only (Fig. 3). The formation of the C_4H_4 intermediate is thermodynamically favorable by 0.82 eV. On $(C_4H_4)/Pd_1/F_{5c}$ the addition of the third acetylene molecule is exothermic by 1.17 eV, leading to a very stable $(C_4H_4)(C_2H_2)/Pd_1/F_{5c}$ intermediate. To transform this intermediate into benzene one has to overcome a barrier of 0.98 eV (Fig. 3). The corresponding energy gain is very large, 3.99 eV, and mainly related to the aromaticity of the benzene ring. Once formed, C_6H_6 is so weakly bound to the supported Pd atom that it immediately desorbs. Thus, the reaction on Pd/ F_{5c} is rate limited in the last step, the conversion of $(C_4H_4)(C_2H_2)$ into C_6H_6 . This is different from the Pd(1 1 1) surface where the rate determining step for the reaction is benzene desorption. The calculations are consistent with the experimental data. In fact, on Pd₁/ F_{5c} the computed barrier of 0.98 eV corresponds to a desorption temperature of about 300 K, as experimentally observed, Fig. 2a. On Pd(1 1 1) surfaces, the bonding of benzene is estimated to be ≈ 1.9 eV (from a BP calculation on a Pd₆/(C_6H_6) cluster). This binding is consistent with a desorption temperature of 500 K as observed for low coverage of C_6H_6 on Pd(1 1 1) [28].

3.2. CO oxidation

First, we verified that the clean MgO(1 0 0) thin films are inert for the oxidation reaction; i.e., no

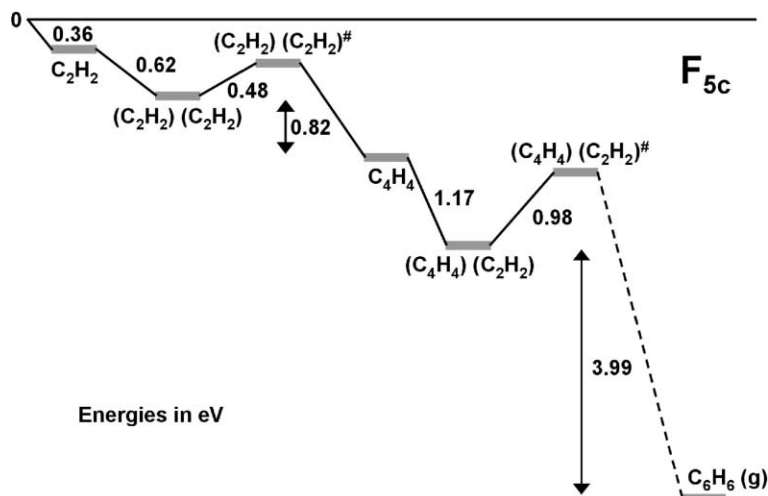


Fig. 3. Energetics of the reaction path for the cyclotrimerization of acetylene to benzene occurring on a Pd atom supported on a F_{5c} center, Pd_1/F_{5c} .

$^{13}C^{16}O^8O$ was formed in a one-heating-cycle experiment after adsorbing $^{18}O_2$ and $^{13}C^{16}O$ (Fig. 4a) or vice versa [29]. When Pd atoms are trapped on the F_{5c} 's, preadsorption of oxygen and subsequent saturation by CO leads to the formation of carbon dioxide, with desorption peaks at 260 K and at around 500 K (Fig. 4c). The existence of two desorption peaks in the TPR spectrum (Fig. 4c) suggests the presence of two different reaction mechanisms. Note that when ^{13}CO is preadsorbed prior to $^{18}O_2$ the oxidation reaction is suppressed, indicating CO poisoning (Fig. 4b).

The calculations were performed using the Born–Oppenheimer (BO) local-spin-density (LSD) molecular dynamics method (BO–LSD–MD) [30] with the generalized gradient approximation (GGA) [31] and employing norm conserving non-local scalar-relativistic [32,33] (for the Pd atom) pseudopotentials [34]. Such calculations yield accurate results pertaining to geometries, electronic structure, and charging effects of various neutral and charged coinage metal clusters [35,36] and nanostructures [37]. The magnesia surface was modelled by a finite region (“cluster”) of atoms, whose valence electrons are treated fully quantum mechanically (using the BO–LSD–MD), embedded in a large (2000 charges) point-charge lattice, as described in recent studies [8].

A single Pd atom binds strongly to the oxygen vacancy (binding energy of 3.31 eV), with a slight amount of charge ($0.15e$) transferred to the adsorbed atom. In comparison, the binding energy of Pd atoms to terrace oxygen sites is only 1.16 eV. The enhanced binding to the F_{5c} is also reflected in the corresponding bonding lengths of 1.65 and 2.17 Å for $MgO(F_{5c})$ –Pd and MgO –Pd, respectively. Binding of two CO molecules saturates the $MgO(F_{5c})$ –Pd system; occupying the $MgO(F_{5c})$ –Pd system with three CO molecules leads to spontaneous (barrierless) desorption of one of the molecules. In the most stable configuration the two CO molecules are inequivalent; one CO binds on top and the second adsorbs on the side of the Pd-atom (this top-side geometry is similar to that shown in Fig. 4I but without the O_2), and the total binding energy of the two CO molecules is 1.62 eV. To study the oxidation mechanisms of CO on $MgO(F_{5c})$ –Pd the system was optimized first with coadsorbed O_2 and two CO molecules. Two stable geometric arrangements were found, with the most stable one shown in Fig. 4I where the CO molecules bind in a top-side configuration and the O_2 is adsorbed parallel to the surface on the other side of the Pd atom. The adsorbed O_2 molecular bond is stretched and activated (1.46 Å compared to the calculated gas-phase value of 1.25 Å). In addition,

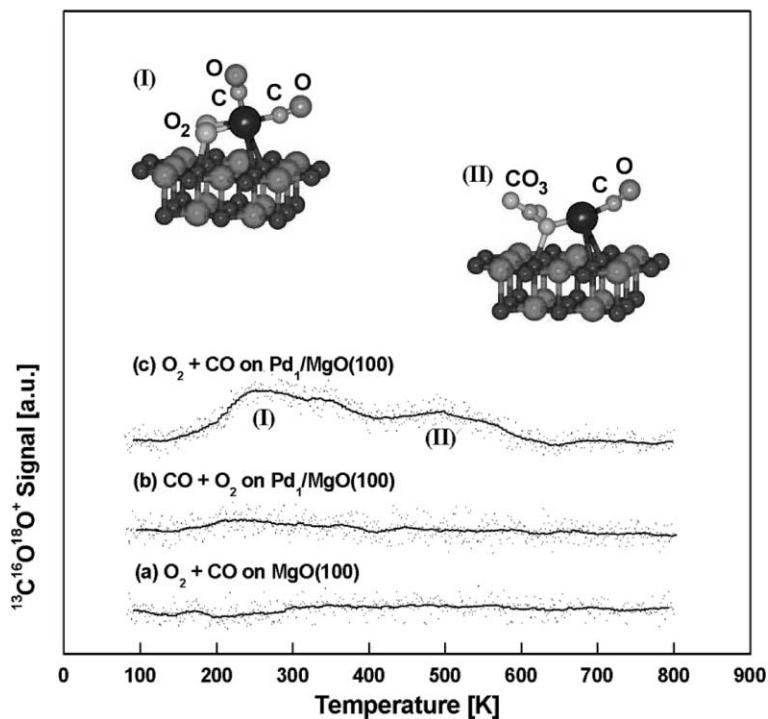


Fig. 4. (a) TPR spectrum of $^{13}\text{C}^{16}\text{O}^{18}\text{O}$ on a clean $\text{MgO}(100)$ film after preadsorption of $^{18}\text{O}_2$ and saturation with $^{13}\text{C}^{16}\text{O}$ at 90 K. Note that no carbon dioxide is formed on these films. (b) TPR spectrum of $^{13}\text{C}^{16}\text{O}^{18}\text{O}$ on a $\text{Pd}_1(0.5\% \text{ ML})/\text{MgO}(100)$ sample after preadsorption of $^{13}\text{C}^{16}\text{O}$ and saturation with $^{18}\text{O}_2$ at 90 K. Note that CO is poisoning the reaction. (c) TPR spectrum of $^{13}\text{C}^{16}\text{O}^{18}\text{O}$ on a $\text{Pd}_1(0.5\% \text{ ML})/\text{MgO}(100)$ sample after preadsorption of $^{18}\text{O}_2$ and saturation with $^{13}\text{C}^{16}\text{O}$ at 90 K. (I–II) Two precursor states ($\text{Pd}/\text{MgO}(\text{F}_{5c})(\text{CO}_3)(\text{CO})$ and $\text{Pd}/\text{MgO}(\text{F}_{5c})(\text{CO})_2(\text{O}_2)$) that precede carbon dioxide formation catalyzed by a palladium atom adsorbed on the $\text{MgO}(100)$ film. The peak (I) of spectrum (c) originates from precursor (I) from the reaction between molecularly adsorbed oxygen and one of the CO molecules (top-CO). The peak (II) of spectrum (c) is due to decomposition of a carbonate complex CO_3 in the precursor (II).

we found a stable carbonate complex $\text{Pd}(\text{CO}_3)(\text{CO})$ (Fig. 4II), whose binding energy is 4.08 eV larger than the aforementioned $\text{Pd}(\text{CO})_2(\text{O}_2)$ complex. These complexes were identified by comparison of calculated and spectroscopically measured CO vibrational frequencies [9]. Two reaction mechanisms are proposed corresponding to the two CO_2 peaks observed experimentally (Fig. 4c). At low temperatures the two relevant precursors are shown in Fig. 4I and II. Corresponding to the 260 K CO_2 desorption peak we propose the following reaction mechanism. In a competitive process, CO desorbs or is oxidized upon heating. The theoretically estimated activation energies of the two processes are 0.89 eV for desorption and 0.84 for oxidation, obtained from a series of constrained

energy minimizations, where the top-CO molecule approaches the closest O atom of the O_2 molecule. Formation of CO_2 at higher temperatures (corresponding to desorption around 500 K, Fig. 4c) involves decomposition of the $\text{Pd}(\text{CO}_3)(\text{CO})$ carbonate complex (Fig. 4II). This mechanism is observed in molecular dynamics simulations where the temperature is controlled to 500 K by Langevin dynamics.

4. Conclusion

Pd atoms adsorbed on F-centers of a $\text{MgO}(100)$ surface are chemically active for the cyclotrimerization of acetylene and the oxidation of

CO. The proposed mechanisms are different than those observed on solid palladium. For the cyclo-trimerization the formation of benzene starting from the intermediate Pd/MgO(F_{5c})(C₄H₄)(C₂H₂) is the rate determining step with an activation energy of 0.98 eV. Due to the Pauli repulsion the product molecule immediately desorbs from the nanocatalyst. In contrast on solid palladium the desorption of benzene is the rate determining step and its activation energy is strongly dependent on the C₆H₆ coverage [28]. For the oxidation of CO, in contrast to bulk palladium [38], the oxygen molecule is not dissociated prior to the reaction and two precursors, Pd/MgO(F_{5c})(CO₃)(CO) and Pd/MgO(F_{5c})(CO)₂(O₂), are involved in the oxidation reaction.

Acknowledgements

This work was supported by the Swiss National Science Foundation (S.A., U.H), the ‘Deutsche Forschungsgemeinschaft’ (U.H), the Italian INFM through the PRA-ISADORA project (A.M.F, L.G, G.P), the U.S. AFOSR (U.L, H.H), and the Academy of Finland (H.H). We thank W.-D. Schneider for his support.

References

- [1] G. Ertl, H.-J. Freund, *Phys. Today* 52 (1999) 32.
- [2] F. Besenbacher, I. Chorkendorff, B.S. Clausen, B. Hammer, A.M. Molenbroek, J.K. Norskov, I. Stensgaard, *Science* 279 (1998) 1913.
- [3] R.L. Whetten, D.M. Cox, D.J. Trevor, A. Kaldor, *Phys. Rev. Lett.* 54 (1985) 1494.
- [4] L. Holmgren, A. Rosen, *J. Chem. Phys.* 110 (1999) 2629.
- [5] A. Berces, P.A. Hackett, L. Lian, S.A. Mitchell, D.M. Rayner, *J. Chem. Phys.* 108 (1998) 5476.
- [6] E.K. Parks, G.C. Nieman, K.P. Kerns, S.J. Riley, *J. Chem. Phys.* 107 (1997) 1861.
- [7] G. Schulze Icking-Konert, H. Handschuh, G. Gantefoer, W. Eberhardt, *Phys. Rev. Lett.* 76 (1996) 1047.
- [8] A. Sanchez, S. Abbet, U. Heiz, W.-D. Schneider, H. Häkkinen, R.N. Barnett, U. Landman, *J. Phys. Chem. A* 103 (1999) 9573.
- [9] S. Abbet, U. Heiz, H. Häkkinen, U. Landman, *Phys. Rev. Lett.* 86 (2001) 5950.
- [10] S. Abbet, A. Sanchez, U. Heiz, W.-D. Schneider, *J. Catal.* 198 (2001) 122.
- [11] U. Heiz, F. Vanolli, L. Trento, W.-D. Schneider, *Rev. Sci. Instrum.* 68 (1997) 1986.
- [12] U. Heiz, *Appl. Phys. A* 67 (1998) 621.
- [13] M.C. Wu, J.S. Corneille, C.A. Estrada, J.-W. He, D.W. Goodman, *Chem. Phys. Lett.* 182 (5) (1991) 472.
- [14] U. Heiz, W.-D. Schneider, *J. Phys. D: Appl. Phys.* 33 (2000) R85.
- [15] S. Abbet, E. Riedo, H. Brune, U. Heiz, A.M. Ferrari, L. Giordano, G. Pacchioni, *J. Am. Chem. Soc.* 123 (2001) 6172.
- [16] A.M. Ferrari, L. Giordano, S. Abbet, U. Heiz, G. Pacchioni, *J. Phys. Chem. B* 106 (2002) 3173.
- [17] R. Ditchfield, W. Hehre, J.A. Pople, *J. Chem. Phys.* 54 (1971) 724.
- [18] P.J. Hay, W.R. Wadt, *J. Chem. Phys.* 82 (1985) 299.
- [19] A.D. Becke, *J. Chem. Phys.* 98 (1993) 5648.
- [20] C. Lee, W. Yang, R.G. Parr, *Phys. Rev. B* 37 (1988) 785.
- [21] A.D. Becke, *Phys. Rev. A* 38 (1988) 3098.
- [22] J.P. Perdew, *Phys. Rev. B* 33 (1986) 8822.
- [23] S. Abbet, A. Sanchez, U. Heiz, W.-D. Schneider, A.M. Ferrari, G. Pacchioni, N. Roesch, *J. Am. Chem. Soc.* 122 (2000) 3453.
- [24] J. Sauer, P. Ugliengo, E. Garrone, V.R. Saunders, *Chem. Rev.* 94 (1994) 2095.
- [25] G. Pacchioni, P.S. Bagus, F. Parmigiani, *Cluster Models for Surface and Bulk Phenomena*, Plenum Press, New York, 1992.
- [26] M.J. Frisch et al., *Gaussian 98*, Gaussian Inc., Pittsburgh, PA, 1997.
- [27] R.M. Ormerod, R.M. Lambert, *J. Phys. Chem.* 96 (1992) 8111.
- [28] W.T. Tysoe, G.L. Nyberg, R.M. Lambert, *J. Chem. Soc., Chem. Commun.* (1983) 623.
- [29] U. Heiz, A. Sanchez, S. Abbet, W.-D. Schneider, *Eur. Phys. J. D* 9 (1999) 35.
- [30] R. Barnett, U. Landman, *Phys. Rev. B* 48 (1993) 2081.
- [31] J.P. Perdew, K. Burke, M. Ernzerhof, *Phys. Rev. Lett.* 77 (1996) 3865.
- [32] L. Kleinman, *Phys. Rev. B* 21 (1980) 2630.
- [33] G.B. Bachelet, M. Schlüter, *Phys. Rev. B* 25 (1982) 2103.
- [34] N. Troullier, J.L. Martins, *Phys. Rev. B* 43 (1991) 1993.
- [35] H. Häkkinen, U. Landman, *Phys. Rev. B* 62 (2000) R2287.
- [36] M. Moseler, H. Häkkinen, R.N. Barnett, U. Landman, *Phys. Rev. Lett.* 86 (2001) 2545.
- [37] H. Häkkinen, R.N. Barnett, A.G. Scherbakov, U. Landman, *J. Phys. Chem. B* 104 (2000) 9063.
- [38] C.J. Zhang, P. Hu, *J. Am. Chem. Soc.* 123 (2001) 1166.